Journal of Phytopathology

WILEY

Journal of Phytopathology

ORIGINAL ARTICLE OPEN ACCESS

Characterisation of *Fusarium* and *Neocosmospora* Species Associated With Crown Rot and Wilt of African Eggplant (*Solanum aethiopicum*) in Ghana

Benjamin Azu Okorley[1] | Sabine Ravnskov[2] | Francis C. Brentu[3] | Samuel K. Offei[4]

[1]Department of Crop Science, College of Basic and Applied Sciences, University Ghana-Legon, Accra, Ghana | [2]Department of Agroecology, Aarhus University Forsøgsvej 1, Slagelse, Denmark | [3]Forest and Horticultural Crop Research Centre, University of Ghana, Kade, Ghana | [4]Biotechnology Centre, College of Basic and Applied Sciences, University of Ghana-Legon, Accra, Ghana

Correspondence: Sabine Ravnskov (sabine.ravnskov@agro.au.dk)

Received: 3 July 2024 | **Revised:** 28 August 2024 | **Accepted:** 29 August 2024

Funding: This research was funded by the Ministry of Foreign Affairs of Denmark through the project 'Building Vegetable Farmers Resilience to Climate Change', DFC project no: 19-04-AU.

Keywords: African eggplant | crown rot | *Fusarium* | *Neocosmospora* | *Solanum aethiopicum* | Wilt disease

ABSTRACT

African eggplant (AEP) (*Solanum aethiopicum* group Gilo) is an important vegetable with considerable economic value in Ghana and tropical Africa. However, fungal diseases threaten its cultivation. Surveys conducted in 2021 and 2022 growing seasons across 35 commercial farms in five regions of Ghana revealed symptoms of crown rot and wilt affecting AEP. This study was undertaken to identify and characterise 36 fungal isolates causing these diseases in AEPs using morphological, molecular and pathogenicity assays. Morphological and molecular analyses of the *Btub2*, *Tef-1α* and *Rpb2* sequences identified two *Fusarium* species (*F. elaeidis* and *F. fredkrugeri*) and three *Neocosmospora* species (*N. falciforme*, *N. suttoniana* and *N. solani*) associated with the plant diseases. *F. elaeidis* (14 isolates) and *N. falciforme* (14) were the most commonly isolated species from symptomatic plants. Specifically, *F. elaeidis* was found in wilting plants, while *F. fredkrugeri* and the three *Neocosmospora* spp. were more associated with wilting plants with crown rot symptoms than plants with only wilt symptoms. All identified species exhibited pathogenicity when inoculated onto AEP roots and stems, confirming field observations. *F. elaeidis* was the most aggressive in inducing wilt symptoms, while *N. solani* and *N. suttoniana* were particularly aggressive in inducing crown rot symptoms. This study is the first to document that *F. elaeidis*, *F. fredkrugeri*, *N. falciforme* and *N. suttoniana* are pathogens causing wilt and crown rot in AEP in Ghana. These findings provide essential insights for developing effective disease management strategies to reduce losses from these fungal species.

1 | Introduction

African eggplant (AEP) (*Solanum aethiopicum*), belonging to the Solanaceae family, is one of the important vegetable crops in Africa. It is an essential nutritional and medicinal resource as well as a valuable rootstock for tomato and eggplant grafting (Han et al. 2021). AEPs are classified into four subgroups based on usage: Gilo, Kumba, Shum and Aculeatum (Han et al. 2021). Gilo type is planted for its edible fruits, Kumba type for edible leaves or fruits, Shum type for edible leaves and Aculeatum for ornamental uses. In Ghana, the Gilo type is widely cultivated and contributes significantly to the local economy as well as foreign exchange through fruit exports to Europe and the United States (Horna, Timpo, and Gruère 2007). However, the crop is susceptible to vascular wilt diseases, which affect plant growth and fruit yield (Owusu et al. 2023).

Research on wilt diseases in eggplants has primarily focused on *S. melongena*, the close relative of AEP (Tassone et al. 2022). The primary disease causing considerable economic losses for *S. melongena* growers has been reported to be wilt caused by *Fusarium oxysporum* f. sp. *melongenae* (*Fom*), *Verticillium dahliae* (Kleb.) or *Sclerotium rolfsii* (Altınok and Can 2010). *Fom* is the most prevalent pathogen in several parts of the world, including Africa, Asia, Europe and the United States (Safikhani, Morid, and Zamanizadeh 2013; Toppino, Valè, and Rotino 2008; Tassone et al. 2022; Altınok and Can 2010). *Fom* can persist in the soil for many years as propagules, saprophytes or colonisers of other plants and then infect eggplant roots when environmental conditions are suitable (Safikhani, Morid, and Zamanizadeh 2013). It colonises the vascular bundles, causing vascular tissue discolouration, leaf wilting, leaf yellowing, defoliation and eventual plant death (Altınok and Can 2010).

In addition to wilt, stem canker caused by *F. solani* (teleomorph: *Nectria haematococca* Berk. & Broome) represents another severe disease impacting the cultivation of *S. melongena* (Cerkauskas 2008). This disease caused an 80% yield loss in greenhouse-produced eggplants in Canada (Cerkauskas 2008).

In recent years, several cases of wilt disease have been reported in AEP fields in Ghana, and it is becoming a significant concern for the industry (Owusu et al. 2023). As a result, control of this disease has gained considerable importance, but reports on fungal pathogens associated with the wilt diseases of AEP are limited. Thus, timely detection and accurate identification of the causal agents are critical for establishing the foundation for epidemiological and disease control investigations.

Numerous morphological, biochemical and DNA techniques are currently available for *Fusarium* detection and identification in vegetables (Crous et al. 2021). The classic plate culture technique and morphological traits (colony pigmentation and growth rate, macro and macroconidia shape and size, chlamydospore type, etc.) are essential for *Fusarium* species recognition (Mui-Keng and Niessen 2003). However, these morpho-characters are often insufficient for confident identification because of cryptic species, morphological homoplasy and phenotypic plasticity (Leslie and Summerell 2006). Instead, DNA sequence analysis in conjunction with morphological studies has become essential for accurate identification (Crous et al. 2021). The internal transcribed spacer (ITS) DNA is the most widely used marker for fungi identification (Schoch et al. 2012), including the phylogeny of *Fusarium* spp. in previous studies (Mui-Keng and Niessen 2003). However, with the emergence of new closely related members within the *Fusarium* species complexes, the ITS was reported as not sufficiently discriminative and unsuitable for resolving the identities of some closely related species (O'Donnell et al. 2022).

In contrast to ITS, analysis of gene sequences such as ß-tubulin, translation elongation factor1-α or RNA polymerase II subunit 2 showed better discriminatory power in phylogenetic resolution and identification of *Fusarium* species at the subspecies levels (Stielow et al. 2015; O'Donnell et al. 2022). Consequently, the taxonomy of *Fusarium* was re-examined with multilocus phylogenetic analyses to support the separation of *F. solani* and its closely related species from *Fusarium* to the genus *Neocosmospora* (Sandoval-Denis and Crous 2018). Additional research into the *F. solani* species complex (FSSC) is needed to fully understand its taxonomic classification as not all species have been formally classified within the genus *Neocosmospora* (Sandoval-Denis and Crous 2018).

This study aims to identify and characterise the fungal species causing wilt and crown rot of AEP (*S. aethiopicum* Gilo group) in the major production areas in Ghana using morphological, molecular and pathogenicity assays. Ultimately, knowledge of the relationship between symptoms and causal agents would improve diagnostic capacity and allow for evaluating management strategies and identifying resistant germplasm.

2 | Materials and Methods

2.1 | Field Survey and Sample Collection

In the 2021 and 2022 growing seasons, plant disease surveys were conducted in 21 major AEP-growing communities distributed across five administrative regions (Central, Eastern, Greater Accra, Western and Volta regions) in Ghana. A total of 35 fields where growers reported wilt incidence were surveyed (see Figure S1 for a map of the study area).

In each community, the prevalence of wilt disease under natural conditions was investigated in one to three fields at least 0.5 km apart. The proportion of plants (%) on which wilt symptoms were observed in an X-shaped path covering an entire field was recorded as the disease incidence. The disease severity was assessed using a 1–6 point scoring scale with slight modification (Boyaci, Unlu, and Abak 2010): 1 = healthy plants; 2 = yellowing of the lower old leaves, < 50% of leaves affected; 3 = yellowing of both young and old leaves, > 50% of leaves affected; 4 = stunting and wilting of older leaves; 5 = severe wilting, both young and old leaves wilted; 6 = dead plant. The average disease incidence and severity were then calculated for each community and region.

2.2 | Isolation of Fungi

Symptomatic plants were collected from each field and transported in a large ice box (1.0 × 0.5 m) to the laboratory for further processing. After thoroughly cleaning the stem and roots with tap water, they were excised laterally to expose tissues beneath the epidermis. Tissue segments, approximately 5 mm^2, were excised from roots and stems and surface disinfested by soaking them in 70% ethanol for 1 min and then in a 2% bleach solution (sodium hypochlorite) for 3 min. The tissues were rinsed thrice in sterile distilled water (SDW) and air-dried under a laminar flow cabinet. Finally, the sample tissues were transferred to Petri dishes containing potato dextrose agar (PDA) amended with 500 mg/L of ampicillin to minimise bacterial growth. The Petri dishes were incubated in the dark at 25°C for 4 days.

The recovered isolates were examined for consistency in their morphology, and as multiple isolates from a field had the same morphology, one isolate was selected to represent the group. The selected isolates were purified using the single spore isolation

method (Leslie and Summerell 2006) and then kept on PDA slant cultures at 4°C until use.

2.3 | Morphological Identification

The fungal isolates were characterised morphologically according to their colony traits and reproductive structures by referring to primary (Leslie and Summerell 2006) and secondary genera and species descriptors (Crous et al. 2021). Mycelia-colonised PDA plugs (5 mm diameter) from a 3-day-old actively growing colony were transferred to fresh PDA in Petri plates (9 cm diameter) and then incubated at 25°C in continuous darkness. After 6 days, the cultural traits of the isolates were differentiated based on colony texture, elevation, margin and pigmentation. The colony diameter (mm) was estimated as the average of two perpendicular measurements taken with a digital Vernier calliper. Each isolate had four replicate cultures, and the experiment was repeated twice.

The micro-morphological traits of the isolates were studied using Spezieller–Nährstoffarmer agar (SNA) medium (1 g KH_2PO_4, 1 g KNO_3, 0.5 g $MgSO_4.7H_2O$, 0.5 g KCl, 0.2 g glucose, 0.2 g sucrose and 15 g agar/L of distilled water) (Crous et al. 2021). Mycelia-colonised PDA plugs were transferred to SNA plates and incubated at room temperature (25 ± 2°C) under ambient fluorescence lighting (12 h photoperiod) for 15 days. The microscopic structures produced were examined in a sterile water medium under a Zeiss Primo Star light microscope (Carl Zeiss Microscopy, GmbH, Germany). An Axiocam 208 high-definition camera (Carl Zeiss Microscopy, GmbH) fitted on the microscope and controlled by Zen (blue edition) software v.3.3 was used to take micrographs and measure spore dimensions. For each isolate, 40 spores were selected randomly for measurement and reported as the mean and range in parenthesis, respectively.

2.4 | Pathogenicity Screening Among Representative Fungal Isolates

2.4.1 | Root Inoculation Assay

The pathogenicity test included 53 fungal isolates representing different farms and isolation sources (Table S1). Their ability to induce wilt symptoms was determined on the AEP commercial cultivar 'Kotobi F1' and two landraces, 'Kade' and 'Maa Narteh'. Fusarium inoculum suspensions, containing 1×10^6 spores/mL, were made from PDA cultures grown at 25°C for 7 days. Spores were dislodged from the colony into suspension by adding 10 mL of sterile distilled water, and the concentration was determined using a haemocytometer.

Ten three-week-old seedlings were inoculated per eggplant genotype/fungal isolate. Seedlings grown in sterilised potting soil were gently removed, and their roots were cleared of soil. Afterwards, the roots were immersed in the spore suspension for 5 min to the crown level (Altınok and Can 2010) and transplanted (at one seedling/pot) into plastic pots containing autoclaved Jiffy substrate (Jiffy Products Int. BV., the Netherlands). Seedlings immersed in SDW were used as the control treatment. Inoculated and control plants were kept in a screen house under ambient conditions.

The experiment was set up using a completely randomised design, with 10 replicate pots for each fungal isolate/eggplant cultivar combination, and the entire experiment was conducted twice. Each time, a Temitope data logger (Elitech Technology, Inc., USA) was used to record the climate conditions inside the screen house. The conditions in the first experiment were 30.4 ± 5.2°C and 72.3 ± 16.7% RH in the day and 23.9 ± 1.5°C and 92.6 ± 5.6% RH at night. The conditions in the second experiment were 28.1 ± 3.3°C and 78.8 ± 11.5% in the day and 23.3 ± 0.6°C and 95.3 ± 2.3% RH at night.

The plants were observed daily for the development of wilt symptoms, and the disease severity (DS) was assessed at 21 days post inoculation (dpi), using a 1–6 point scoring scale described previously (Boyaci, Unlu, and Abak 2010). At 23 dpi, root and stem tissue segments excised from symptomatic plants were surface sterilised in a 2% bleach solution for 3 min, rinsed with SDW and then transferred to PDA for pathogen re-isolation. Five days after incubation, the recovered isolates were identified morphologically and compared with the original isolates to satisfy Koch's postulates.

2.5 | DNA Extraction and PCR Amplification

The genomic DNA of the 36 pathogenic isolates was extracted from 5-day-old cultures and grown on PDA overlaid with a cellophane membrane. Approximately 20 mg of mycelia was ground in liquid nitrogen to fine powder, and the total DNA was extracted using a Quick-DNA MiniPrep Kit (Zymo Research Corp., California, USA) according to the manufacturer's guide. Three gene regions, namely, partial sequences of the beta-tubulin (*Btub2*), translation elongation factor 1-*alpha* (*Tef-1α*) and RNA polymerase second-largest subunit (*Rpb2*), were targeted to confirm species identity. The genes were amplified with the following primer pairs Bt2a and Bt2b (Glass and Donaldson 1995), EF1 and EF2 (O'Donnell et al. 1998), and 5F2 and 7cr (Reeb, Lutzoni, and Roux 2004; Liu, Whelen, and Hall 1999) (Table S2), respectively, in a DNA Engine Tetrad 2 Thermal Cycler (Bio-Rad Lab., Inc., USA).

A 25 μL reaction mixture containing 2.5 μL of 10× PCR reaction buffer, 0.6 μL of 10 mM dNTP mix, 2 μL of $MgCl_2$ (4 mM), 1 μL of each 0.5 mM primer (forward and reverse), 3 μL of 20–30 ng genomic DNA template, 0.3 μL of 1 U Taq DNA polymerase (Roche, Basel, Switzerland) and 14.6 μL of dd H_2O was used. The PCR amplification cycle for *Btub2* was tuned to initial denaturation at 95°C for 4 min, followed by 35 cycles at 95°C for 1 min, annealing at 52°C for 30 s, initial extension at 72°C for 1 min and final extension at 72°C for 10 min. Similar amplification conditions were used for the other genes but at different optimal annealing temperatures (Table S2). The amplified products were run on a 1.5% agarose gel electrophoresis and then visualised with a Gel Doc imaging system (Bio-Rad Lab., Inc., USA). After cleaning the DNA bands with the ExoSAP-IT Cleanup Reagent (Thermo Fisher Scientific, USA), the purified PCR products were sequenced in both directions at Macrogen Inc. (Seoul, South Korea).

2.6 | Phylogenetic Analysis

To create a consensus sequence, the forward and reverse sequences obtained were checked and aligned in BioEdit v.7.2.5 (Hall 1999). The newly generated sequences of each gene/isolate were deposited in GenBank (Table S3). Next, Blastn pairwise analysis was performed in the FUSARIOID-ID database (Crous et al. 2021) and type specimen database at NCBI (http://blast.ncbi.nlm.nih.gov/Blast.cgi), respectively, using the *Tef-1α*, *Rpb2* and *Btub2* sequences to determine the closest phylogenetic relatives of the present Ghanaian isolates. Based on the pairwise analysis, 17 reference strains (Table S3) were retrieved from GenBank and included in the multiple alignment dataset. These reference strains are widely recognised species of *Fusarium* and *Neocosmospora* with phylogenies published by Lombard et al. (2019) and Sandoval-Denis and Crous (2018).

Sequence alignments were performed separately for each *gene* using the ClustalW program (Thompson, Higgins, and Gibson 1994). Afterwards, the flanking and ambiguously aligned regions were trimmed in the Gblocks 0.91b package (Dereeper et al. 2008), using the less stringent criteria for selecting conserved blocks. Phylogenetic trees for the aligned sequences were determined by maximum likelihood (ML) and Bayesian inference (BI) analyses.

The ML analysis was performed on the IQ-TREE v.1.6.12 web portal (Nguyen et al. 2015) utilising a concatenated matrix created by merging the *Tef-1α*, *Rpb2* and *Btub2* sequences in the Fabox joiner web portal (Villesen 2007). The best-fit nucleotide substitution model, Tamura and Nei (TNe) + Gamma distribution (+*G*) (Tamura and Nei 1993), was deduced for the data based on the Bayesian information criterion (BIC) in JModelTest 2.1.10 (Darriba et al. 2012). The robustness of ML tree branches was verified by bootstrapping with 1000 replicates, while further assessment of branch support was performed with the ultrafast bootstrapping method (UFBoot2 tool; Hoang et al. 2018).

Further, BEAST v.1.8.4 software package (Drummond et al. 2012) was used for the BI analysis, and each gene sequence was handled as a separate partition with a unique nucleotide substitution model: GTR + G for *Tef-1α* and TNe + G for *Rpb2* and *Tub2*. Two independent Markov Chain Monte Carlo (MCMC) runs starting with a UPGMA tree were made for 10 million generations, with trees sampled every 1000 generations. The initial 1000 trees from each run were discarded as burn-in, and the BI posterior probabilities were estimated from the remaining (18,000) trees. The trees were visualised in Figtree v.1.4.4 (http://tree.bio.ed.ac.uk/software/figtree/), and the BI posterior probabilities (%) were included in the ML phylogram.

2.7 | Stem Inoculation Assay

A further test to evaluate the pathogenicity of fungal species on the stems of Kotobi F1 and Kade seedlings was conducted following the methods described in a recent study (Sandoval-Denis et al. 2018). Three randomly selected isolates from the five fungal species were used for the study, except *F. fredkrugeri*, with one isolate, Dzod03. Seedlings were raised as described above, and the transplants were maintained in pots for 6 weeks till the stems developed hardwood tissues/lignified. The stems were inoculated at approximately 3–4 cm aboveground level with a mycelial plug (8 mm diameter) taken from a 7-day-old actively growing colony on PDA. Pathogen-free PDA plugs were used for control plants. Four potted plants of each eggplant cultivar were inoculated for each fungal isolate and then wrapped with a strip of parafilm (Bemis Co. Inc., Wisconsin, USA) to avoid desiccation.

The experiment was conducted using a completely randomised design with four replicates. The entire experiment was repeated once using wounded stems. A small cut, approximately 3 mm long, was made on the stems using a sterile scalpel to remove the outer epidermal layer before the agar plug was inserted and wrapped with a parafilm strip. Inoculated plants and controls were incubated in a screen house under ambient weather conditions: 30.4 ± 5.2°C and 23.9 ± 1.5°C average day and night temperatures; 72.3 ± 16.7% and 92.6 ± 5.6% average day and night RH, respectively.

Ten days post inoculation, the external lesion length on stems was measured and visually rated based on the extent of tissue discolourations and shoot symptoms as follows: 0 = healthy plants with no stem discolourations; 1 = weak stem rot lesions, with sparse pale brown discolourations; 2 = moderate rot lesions, with dark discolourations, stem girdling and leaf chlorosis; 3 = severe rot lesions, resulting in extensive stem tissue discolouration, desiccation, cracks and partial wilting of leaves; 4 = extremely severe rot lesions, resulting in rapid wilt or shoot dieback; and 5 = dead plant (Cerkauskas 2008). The inoculated fungi were reisolated from stems with crown rot lesions and identified morphologically, as described previously, to fulfil Koch's postulates.

2.8 | Host Range Assays

One isolate/fungal species was randomly chosen to assess their cross-pathogenicity on Chilli pepper (*Capsicum frutescens*) cv. 'Legon 18', bell pepper (*Capsicum annuum*) cv. 'Yellow Wonder' turkey berry (*S. torvum*), tomato (*S. lycopersicum*) cv. 'Pectomech' and *S. macrocarpon* ('Gboma'), African eggplant cv. 'Kade'.

The fungal inocula and inoculation methods used in the host range assays were similar to those used in the previously mentioned experiments. Seedlings were raised in pots filled with Jiffy potting mix. Three-week-old seedlings were root-dip inoculated with fungal spore suspension for the wilt test, and 6-week-old seedlings were inoculated with mycelia plugs for the crown rot test. Five seedlings/host were treated and placed in the screen house for each fungal species. Control treatments consisted of seedlings inoculated with sterile H_2O.

The screen house conditions for the first experiment were, on average, 31.7 ± 4.2°C and 24.3 ± 1.8°C, 66.2 ± 15.3% RH and 89.3 ± 6.0% RH, respectively, during the day and night hours. Also, the conditions in the second experiment were

30.8 ± 4.5°C and 24.5 ± 1.4°C; 75.3 ± 14.1% RH and 93.1 ± 7.2% RH, respectively, during the day and night hours. The crown rot and wilt symptomatic plants were evaluated qualitatively (presence/absence) at 10 and 21 dpi, respectively. Re-isolation and identification of the inoculated fungi from plants with crown rot lesions and wilt symptoms were performed to satisfy Koch's postulates.

2.9 | Statistical Analysis

Data obtained from morphological study and pathogenicity experiments were analysed using the Genstat V12 statistical package (VSN Int., Hempstead, UK). The data were checked for normality, and Bartlett's test was performed to show the homogeneity of variances between repeated experiments. When the results revealed no significant interaction or similarity of variances between the repeated experiments, the data were merged for further analysis.

An analysis of variance test was performed to determine differences in DS and lesion length between species, isolates within species and cultivars. In addition, the relative importance of each factor to the total variance in DS was estimated using the variance decomposition technique. Pairwise comparisons were made to separate statistically significant means using Tukey's HSD test at $\alpha = 0.05$. Nonpathogenic fungal isolates were classified as any treatment that did not result in a statistically significant difference compared to the control.

3 | Results

3.1 | Symptoms and Prevalence of Wilt in African Eggplant

Visual examination of affected fields showed vascular wilt as the most prevalent disease, with plants displaying symptoms such as leaf yellowing, wilting and premature defoliation (Figure 1a). Secondary symptoms included light to dark-brown vascular discolourations and brown streaks in the crown and belowground parts of stems, which could be visualised after cutting them open (Figure 1b,c). The disease affected the plant throughout its entire growth and fruiting stages. Severely infected plants wilted and died at the vegetative stage or during the first fruiting stage. In contrast, the moderately infected plants survived infections during the growing season but appeared severely stunted with systemic chlorosis.

Wilting plants also showed stem rot symptoms close to the soil line (Figure 1d–f). These plants had decaying tan-brown or black necrotic lesions around the main stem, spreading to one or more aboveground branches (Figure 1e,f). Eventually, the infected plants developed leaf chlorosis, wilted and died. Cream to orange-coloured spore masses formed on the surfaces of the damaged bark tissues under wet conditions.

The disease incidence varied among the regions surveyed, ranging from 20% to 39% (Table 1). Disease incidence and severity were generally high in communities in the Eastern and Western regions and lower in the Greater Accra regions.

3.2 | Fungal Isolation

One hundred and sixty-four plant samples collected from fields displayed characteristic wilt symptoms, while 121 samples displayed both wilt and crown rot symptoms. Through isolation and culturing, 274 fungal isolates were obtained from the samples. Based on the preliminary morphological evaluation from each farm, duplicate isolates were eliminated, and 53 representative isolates were chosen for pathogenicity screening (Table S1). Thirty-six of the fungal isolates found to be pathogenic on AEP were considered for further testing in this study. Living cultures of the isolates were deposited in the Forest and Horticultural Crop Research Centre, Plant Pathology Herbarium, UG, Ghana.

3.3 | Morphological Identification of Pathogenic Isolates

The morphological characteristics of the 36 pathogenic isolates on PDA and SNA were similar to fungi belonging to the genera *Fusarium* and *Neocosmospora* (formally known as *Fusarium solani* species complex). The morphological characteristics of the various species were characterised (Table S4). Two *Fusarium* species (*F. elaeidis* and *F. fredkrugeri*) and three *Neocosmospora* species (*N. falciforme*, *N. suttoniana* and *N. solani*) were identified using the *Fusarium* species identification keys (Sandoval-Denis and Crous 2018; Lombard et al. 2019; Crous et al. 2021).

Fusarium elaeidis isolates showed morphological markers typical of members of the *Fusarium oxysporum* species complex (FOSC) (Lombard et al. 2019). Colonies on PDA in the dark at 25°C are fast-growing, averaging 81.25 ± 0.41 mm diameter after 6 days; they appeared greyish white, with pale beige regular margins and abundant floccose aerial mycelium. Colonies produced distinct pink or light purple pigments on the top and bottom sides of plates (Figure 2a). Microconidia produced on SNA are unicellular, occasionally with 1-septate, hyaline, oval or slightly curved: av. ± SD 9.82 ± 1.74 × 3.93 ± 0.56 µm. The sporodochia are rosy buff to pale orange to salmon and contain macroconidia that are typically curved or falcate, with parallel walls tapering towards both ends, apical cells curved with a blunt to papillate tip and a poorly developed foot-like basal cell; they are 2–3 septate, hyaline, smooth- and thin-walled: 34.90 ± 2.71 × 5.56 ± 0.51 µm. Chlamydospores were few in mycelium, globose to subglobose, slightly verrucose and thick-walled, formed terminally on hyphae or conidia, and mostly solitary or in pairs.

Fusarium fredkrugeri colonies after 6 days on PDA averaged 79.23 ± 0.63 mm with an even advancing margin. Their surfaces were felty, initially cream-coloured, later turning pale brown, with abundant aerial mycelium. They produced reddish brown to blood sepia pigment in the top and reverse side of the petri dish, which is typical of this fungal species (Sandoval-Denis, Swart, and Crous 2018) (Figure 2b). On SNA, colonies were flat with scanty aerial mycelium; microconidia formed in false heads were unicellular smooth-walled, hyaline, obovoid, ellipsoidal to allantoid: 5.08 ± 0.50 × 2.77 ± 0.29 µm. Sporodochia and macroconidia were not found in any agar media.

Fusarium falciforme colonies grew moderately fast on PDA, reaching an average of 74.61 ± 0.95 mm after 6 days, with smooth

FIGURE 1 | Infected African eggplants (*Solanum aethiopicum* group Gilo) displaying vascular wilt (a–c) and crown rot symptoms (d–f) in the field. (a) Wilting of plants at the fruiting stage, leading to extensive defoliation and plant death. (b) A longitudinal section of a stem showing discolourations of vascular bundles and brown streaks. (c) Cross-section of stem showing the outgrowth of suspected fungal pathogen beneath the epidermis. (d) Wilting in plants with crown and stem rot symptoms. (e) Close view of rotten stem tissues around soil line. (f) Progression of infection towards the branches (arrows indicate the colonised tissues and spores of the suspected agent).

TABLE 1 | Number of fields, wilt incidence and severity during the survey of African eggplant fields in Ghana.

Location	No. of communities or towns	No. of fields	Mean incidence (%)	Severity (1–6)
Region				
Central	4	5	27.50 ± 8.54[a]	4.38 ± 0.24
G-Accra	1	1	20.00 ± 2.25	3.25 ± 0.21
Volta	6	10	30.64 ± 6.68	4.03 ± 0.54
Eastern	7	14	39.00 ± 2.19	5.17 ± 0.25
Western	3	5	38.33 ± 3.33	5.56 + 0.29
Overall	21	35	33.42 ± 2.73	4.66 ± 0.23

[a]Mean ± standard error.

and regular advancing edges; they had a distinctly white, felty to cottony aerial mycelia, with limited pigments in the top and reversed side of the petri dish (Figure 2c). On SNA, the colonies sporulated abundantly from cream-coloured sporodochia and directly from conidiophores formed on mycelia. Microconidia formed in false heads are hyaline, 0–1 septate, oblong, ellipsoidal, or reinform, and measured 12.38 ± 1.77 × 4.74 ± 0.64 μm. The species was distinguished from the other *Neocosmospora* species by their sickle-shaped macroconidia, bent more towards the blunt apical cells. They were hyaline, typically 3 septate (occasionally 4 septate), with a papillate and nonfoot-shaped basal cell: 41.02 ± 2.21 × 6.87 ± 0.56 μm.

For *N. suttoniana*, colonies grew slowly on PDA, reaching an average size of 71.57 ± 1.78 mm after 6 days. Their surfaces were pale luteous to rose buff-coloured, subfelty to velvety with abundant short white aerial mycelium; the reverse sides were pale sulphur yellow (Figure 2d). On SNA, colonies formed

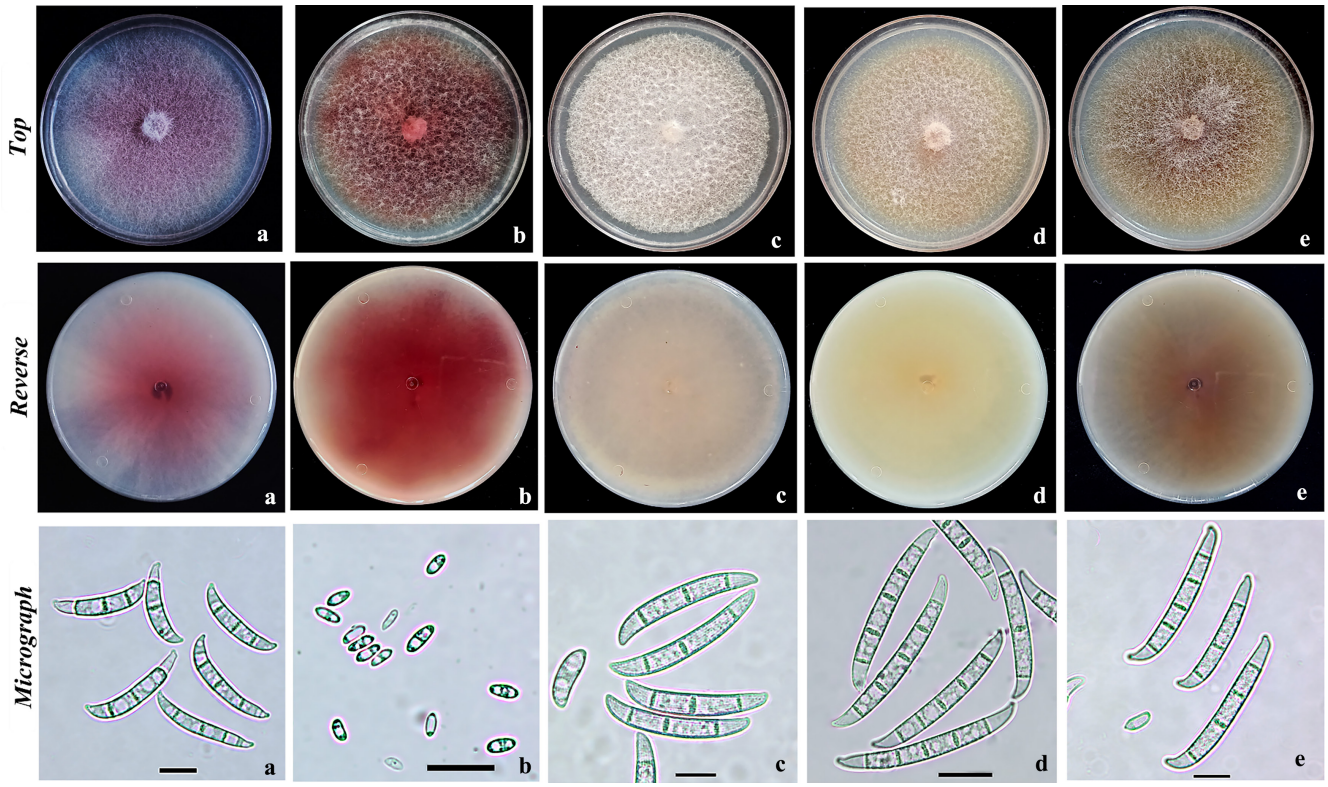

FIGURE 2 | Morphology and cultural characteristics of *Fusarium* and *Neocosmospora* spp. recovered from African eggplant samples. The top panel in each column represents the top, and the middle panel represents the colony's reverse side on PDA after 6 days. The lower panel is the micrographs of macroconidia (a, c, d and e) and microconidia (b) of the fungal species. *Fusarium elaeidis* (a), *F. fredkrugeri* (b), *N. falciforme* (c), *N. suttoniana* (d) and *N. solani* (e). Bars = 20 μm.

dark cream sporodochia, interspersed by a few green-coloured ones. Microconidia were hyaline, 0–2 septate, cylindrical, obovoid, or ellipsoid, 11.76 ± 1.58 × 4.58 ± 0.51 μm. Macroconidia were hyaline, straight with a moderate dorsal curvature that is prominent in the apical and basal thirds, 3–5 septate, 53.23 ± 2.87 × 6.62 ± 0.32 μm; apical cell blunt and elongated, basal cell papillate to barely notched.

N. solani colonies grew slowly, reaching an average of 67.69 ± 3.12 mm after 6 days on PDA. They had pale brown mycelium with regular margins and abundant floccose to cottony aerial mycelium. The brown to brownish olive pigmentations on the top and bottom of the petri dish distinguished this species from the others (Figure 2e). On SNA, colonies formed cream sporodochia interspersed with a few bluish-green ones. Macroconidia were straight and wide in the centre of their length, 3–5 septate, 45.01 ± 3.66 × 6.16 ± 0.48 μm; apical cells were hooked shaped with a blunt rounded end; basal cells were notched or foot-shaped. The microconidia ranged from oval, reinform and cylindrical to occasionally obovoid with a truncated base and 0–1 septate: 9.95 ± 1.65 × 3.84 ± 0.63 μm. Chlamydospores were sparse and formed intercalary on hyphae, occurring singly or in clusters, primarily globose or subglobose with rough walls.

3.4 | Identification-Based on DNA Sequencing

Targeted regions from all isolates were successfully amplified, except for the *Rpb2* sequences of five isolates, which failed after multiple attempts. The 103 sequences obtained (36 *Btub2*, 36 *Tef-1α* and 31 *Rpb2*) were deposited in GenBank (Table S3).

BLASTn analyses in the nucleotide databases at the FUSARIUM-ID (Crous et al. 2021) and NCBI revealed a 98%–100% similarity for *Tef-1α*, 99%–100% similarity for *Rpb2* and 94%–100% similarity for *Btub2* with validly reported sequences *of Fusarium* and *Neocosmospora* species (Table S1). The *Tef-1α* sequences identified 14 isolates as *F. elaeidis*, 1 as *F. fredkrugeri*, 14 as *N. falciforme*, 3 as *N. solani*-melongenae (formally referred to as *N. ipomoeae* (Halst.) L. Lombard & Crous) and 4 as *N. suttoniana*. Analysis of the *Rpb2* sequences supported the classification based on *Tef-1α*, except for five isolates whose *Rpb2* amplification failed in PCR. Further analysis with *Btub2* sequences did not sufficiently or consistently support the classification based on *Tef-1α* or *Rpb2*. For example, isolates identified as *N. falciforme* and *N. suttoniana* were all identified as *N. falciforme* based on *Btub2* sequences.

3.5 | Phylogenetic Inference

A total of 1746 bp alignments (*Tef-1α*: 1–651; R*pb2*: 652–1463; *tub2*: 1464–1746) between 36 isolates from AEPs and 17 reference isolates from GenBank were processed, of which 443 sites were parsimony informative and 1213 were constants. The phylogenetic trees resulting from IQtree-ML and BI analyses of the combined dataset had similar topologies. Hence, only the ML tree is shown in Figure 3 with the ML bootstrap (ML-BS), Bayesian posterior probabilities (BPP) and UltraFast bootstrap

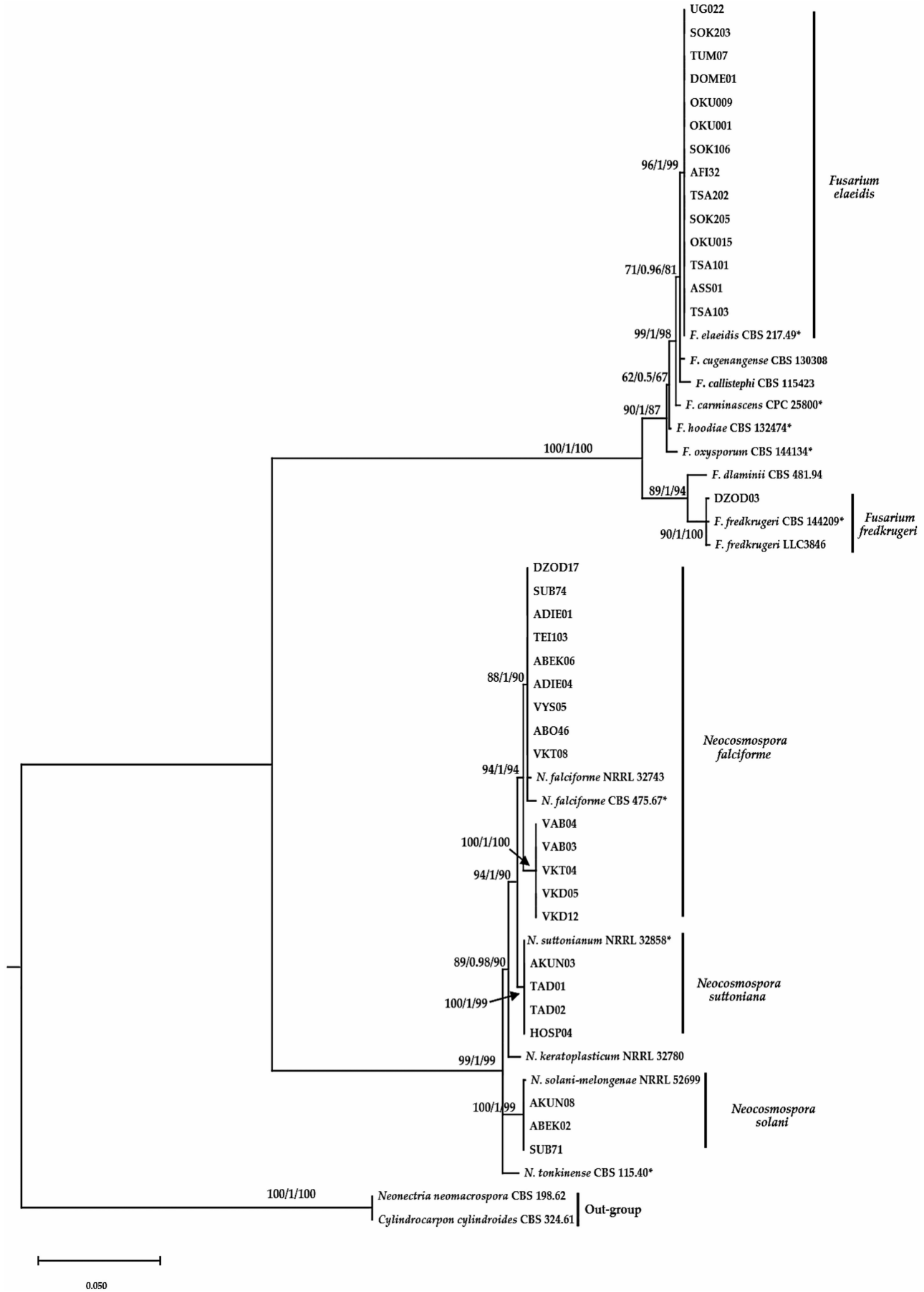

FIGURE 3 | Legend on next page.

FIGURE 3 | Maximum-Likelihood (IQ-TREE-ML) consensus tree obtained by analysis of the combined *Tef-1α*, *Rpb2* and *Btub2* sequence alignments of the genera *Fusarium* and *Neocosmospora*. Values on branches represent Maximum Likelihood (ML-BS), Bayesian posterior probabilities (BP) and ultraFast (UFboot-BS) bootstrap support values above 70%, 0.70%, 80%, respectively. *Neonectria neomacrospora* and *Cylindrocarpon cylindroides* were used as outgroups. The reference strains were retrieved from the collections of the Westerdijk Fungal Biodiversity Institute, Utrecht, the Netherlands (CPC), and the Agricultural Research Service, Peoria, IL, USA (NRRL). The scale bar indicates substitutions per site. Ex-type strains are marked with *.

(UFboot-BS) support values indicated above the branches (see Figure S2 for the BI tree).

The ML and BI analyses successfully classified the 36 isolates in this study into five phylogenetic species supported by high bootstrap values (ML, BPP and UFboot-BS values > 85%, 0.98 and 90%, respectively). Two species resided in the genus *Fusarium* and three in *Neocosmospora*. Fourteen fungal isolates from plants showing only wilt symptoms clustered strongly with the reference isolate from oil palm, *F. elaeidis* (CBS17.49). One isolate (Dzod03) from plants showing crown rot and wilt symptoms clustered with *F. fredkrugeri* (CBS 144209). The remaining 21 isolates belonged to the genus *Neocosmospora*. Fourteen were classified as *N. falciforme*, four as *N. suttoniana* and three as *N. solani*.

3.6 | Number of Fungal Isolates/Species and Distribution in Fields and Regions

The study observed that in 34 out of the 35 fields surveyed, the fungal species occurred alone. However, in one field, both *F. fredkrugeri* and *N. falciforme* were found to coexist on different plants in the same field. *F. elaeidis* was found in 14 fields (Figure 4a). *N. falciforme* was present in 14 of the fields, while *N. suttoniana*, *N. solani* and *F. fredkrugeri* were present in four, three and one field, respectively.

The most commonly isolated fungal species were *F. elaeidis* with 14 isolates and *N. falciforme* with 14 isolates, respectively ($N_{isolates} = 36$) (Figure 4b). However, their distribution varied among AEP production areas. *F. elaeidis* was widespread in four regions: Eastern, Central, Western and G-Accra (Figure 4c). In contrast, *N. falciforme* was limited to the Eastern, Western and Volta regions. Interestingly, in the Volta region, where *F. falciforme* was more abundant, *F. elaeidis* was absent.

Concerning the source of isolation, all 14 isolates of *F. elaeidis* were recovered from plants that displayed only wilt symptoms (Figure 4d). However, 15 isolates of the three *Neocosmospora* spp., along with *F. fredkrugeri*, were more often than not recovered from wilting plants with crown rot than from plants with only wilt symptoms (seven isolates).

3.7 | Pathogenicity of the Fungal Isolates

3.7.1 | *Fusarium* Wilt Test

The results of the pathogenicity test revealed that 36 fungal isolates out of 53 were pathogenic on the eggplant seedlings. First, an initial yellowing from the first and second leaves of all the infected plants was observed among all the fungal treatments. However, as the infection progressed, there were marked distinctions between the symptoms presented in plants treated with *F. elaeidis* and the other four fungal species (Figure 5a, iii vs. ii). *F. elaeidis* inoculated plants showed typical wilt symptoms; most of the plants lost their leaves and died top-down at 21 dpi (Figure 5a, iii and Figure 5b). The mock-inoculated plants did not develop any symptoms (Figure 5a, i).

In contrast to *F. elaeidis*, plants treated with *F. fredkrugeri* and the three *Neocosmospora* species generally appeared severely stunted with small-sized chlorotic leaves relative to the control plants at 21 dpi (Figure 5a, ii). Wilt symptoms developed in these plants only when there was evidence of root and stem rot around the crown region (Figure 5c–f). These species induced brown to black rot lesions on the roots, crown and stems; plants with soft stem tissues collapsed and died. *N. solani* produced orange-coloured perithecia containing ascospores on the host substrate (Figure 5f–h). Fungal isolates with identical morphologies as those inoculated initially were reisolated from the diseased plants but not from the healthy control plants, which confirmed Koch's postulates.

3.7.1.1 | Virulence Comparison. The DS between repeated experiments was similar (experiment $1 = 3.95 \pm 1.45$; experiment $2 = 3.86 \pm 1.38$; $p = 0.089$) based on Bartlett's test for variance homogeneity. As a result, data from both experiments were combined for further analysis. The ANOVA test showed differences in DS depending on fungal species, isolates within species, cultivars as well as their interactions ($p < 0.001$) (Table S5). This notwithstanding, pathogen species contributed the most (50.7%) to the total variance in DS, even more than isolate (23.2%), cultivar (1.0%), species × cultivar interaction (1.0%) and isolate × cultivar interaction (6.5%).

Fusarium elaeidis had the highest DS (5.08) at 21 dpi and was classified as highly virulent relative to the other fungal species. *N. solani* (DS = 3.79) was classified as moderately virulent, whereas *N. suttoniana* (3.26) and *N. falciforme* (3.24) were classified as having somewhat low to moderate virulence. *F. fredkrugeri*, with a DS of 2.45, showed the lowest virulence. Accession Kade was more susceptible to wilt (4.08) than Kotobi (3.90) and Maa-Narteh (3.73). Overall, the symptoms obtained in the artificial inoculation test matched those observed under field conditions. It showed that *F. elaeidis* causes vascular wilt, whereas *F. fredkrugeri* and the *Neocosmospora* spp. contributed to wilts by causing crown and root rots.

3.7.2 | Crown Rot Test

To confirm the fungal species causing crown rot without ambiguity, whole and wounded stems were inoculated with mycelia plugs from 13 fungal isolates. All the isolates tested were

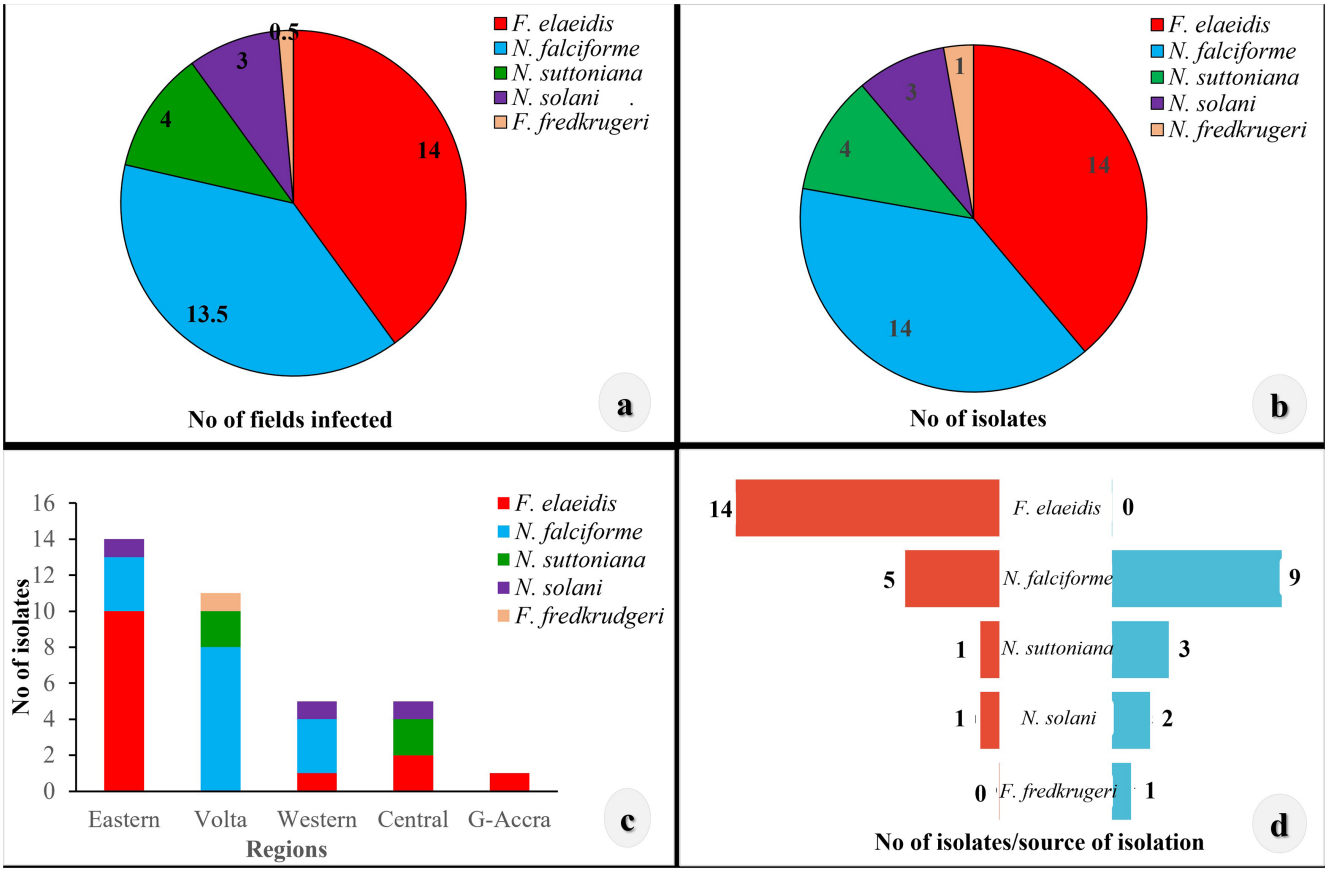

FIGURE 4 | Number of fungal isolates/species and their distribution in African eggplant-growing regions of Ghana. (a) Number of fields infected by fungal species. (b) Number of isolates in each fungal species. (c) Distribution of fungal species across regions. (d) The number of isolates recovered from plants with different symptoms: Wilt only versus wilting with crown rot.

pathogenic and induced necrotic lesions on stems, resulting in stem girdling, wilting of leaves and plant death (Figure 6).

At 10 dpi, differences in stem discolouration ($p = 0.548$) and lesion length ($p = 0.589$) between experiments (i.e., inoculated whole stems versus wounded stems) were not significant according to Bartlett's test. Consequently, data from both experiments were combined for the ANOVA test. The results showed that stem discolouration and lesion length were highly variable between the fungal isolates and between species, indicating varying degrees of pathogen aggressiveness (Table S6). The most severe symptoms, resulting in the death of plants at 10 dpi, were caused by the isolates Abek02, Sub71 and Akon03. These highly aggressive isolates produced intense rotten textured lesions ranging from 31.99 to 39.57 mm. In comparison, isolates Oku15, TSA101 and UG022 were weakly aggressive, causing slight and spotty necrotic lesions ranging from 10.01 to 17.49 mm in size.

Further, data from the two experiments, isolates, replications and host genotypes were averaged to focus on differences in aggressiveness among fungal species (Table S6). The isolates of *N. solani* were the most aggressive, followed by *N. suttoniana* and *N. falciforme*. *F. elaeidis* isolates were the least aggressive on the stems.

3.8 | Host Range Test

The host range of five fungal isolates as wilt and crown rot pathogens was assessed across five *Solanum* species. Following root inoculation, it was observed that the five isolates were not pathogenic on turkey berry and tomato seedlings (Table 2). In contrast, isolate Dzod03 of *F. fredkrugeri* and Abek02 of *N. solani* induced chlorosis and wilt symptoms in chilli and bell peppers. Furthermore, wilt symptoms in *S. macrocarpon* were induced by Oku015 of *F. elaeidis*, Abek02 of *N. solani* and Adie04 of *N. falciforme*. All five fungal isolates caused wilt symptoms in AEP (Kade), consistent with their pathogenicity in earlier pathogenicity tests.

Apart from the wilt test, evaluation of the fungal isolates on the stems revealed some degree of structural specificity to host organs/tissues. For example, the fungal isolates that could not infect the host via its roots could infect the same host via the stem tissues.

The five fungal isolates were pathogenic on the stems of all the host plants, except for interactions between isolate Adie04 and bell pepper, where the host showed no symptoms. The symptoms manifested by the host plants were more or less similar. The initial pale brown lesions gradually turned necrotic and spread to

FIGURE 5 | Vascular wilt and crown rot symptoms in artificially inoculated seedlings of three African eggplant genotypes. (a) A photograph comparing symptoms expressed in *Fusarium elaeidis* treated plants (iii) and other pathogenic species (ii) to the control plants (i) at 21 dpi. Symptoms produced in plants treated with *Fusarium elaeidis* (b), *F. fredkrugeri* (c), *Neocosmospora falciforme* (d), *N. suttoniana* (e) and *N. solani* (f). Perithecia (g) and ascospores (h) of *Nectria haematococca* (teleomorph of *N. solani*) on a stem with crown rot. Scale bar in micrograph (i) = 20 μm.

encircle the stems or had a rotting texture. Abek06 of *N. solani* and Akun03 of *N. suttoniana* exhibited severe symptoms that resulted in plant mortality at 7 dpi, regardless of the host. Each host showed consistent responses across replicates, with their control plants displaying no symptoms. Morphological comparisons confirmed that the reisolated fungi from the symptomatic plant tissues were identical to the original inoculated fungal species.

4 | Discussion

Wilt disease is a significant challenge to AEP production in Ghana, impacting yield and quality (Horna, Timpo, and Gruère 2007; Owusu et al. 2023). This study isolated and characterised 36 pathogenic fungal isolates from the AEP Gilo group, showing wilt symptoms in five regions. The findings revealed a widespread incidence and distribution of the disease, indicating its significant presence throughout the areas surveyed. Using morphological identification, multigene phylogenetic analysis and pathogenicity testing, two species of *Fusarium* (*F. elaeidis* and *F. fredkrugeri*) and three species of *Neocosmospora* (*N. falciforme*, *N. suttoniana* and *N. solani*) were identified as the causal agents of wilt in AEP in Ghana.

Previously, many microbes, including the bacterium *Ralstonia solanacearum*, and fungi including *Fusarium* spp., *Macrophomina phaseolina* and *Verticillium dahliae*, were identified to cause wilt disease in eggplants (Xu et al. 2024; Safikhani, Morid, and Zamanizadeh 2013; Toppino, Valè, and Rotino 2008). In particular, *F. oxysporum* f. sp. *melongenae* has been recognised as the primary pathogen affecting European eggplants (*S. melongena*) globally (Altınok and Can 2010). In a study by Owusu et al. (2023), eight *Fusarium* species (*F. culmorum*, *F. accuminatum*, *F. oxysporum*, *F. proliferatum*, *F. solani*, *F. poae*, *F. subglutinans* and *F. verticillioides*) were identified from AEP in three regions of Ghana. However, the current investigation revealed the existence of pathogens previously unknown as causative agents of wilt disease in AEP, thereby advancing our understanding of fungal pathogens associated with wilt disease.

FIGURE 6 | Crown/stem rot symptoms produced after artificial inoculation of African eggplant stems with pathogen-free PDA plugs (control) (a), *F. elaeidis* (b), *F. fredkrugeri* (c), *N. falciforme* (d), *N. suttoniana* (e) and *N. solani* (f). Bars = 20 mm.

TABLE 2 | Development of wilt and crown rot symptoms in the host range test.

	F. elaeidis	*F. fredkrugeri*	*N. solani*	*N. falciforme*	*N. suttoniana*
Wilt development at 21 days after root inoculation					
Chilli pepper (Legon 18)	N	Y	Y	N	N
Bell pepper (Yellow wonder)	N	Y	Y	N	N
Turkey berry (*S. torvum*)	N	N	N	N	N
Tomato (Pectomech)	N	N	N	N	N
S. macrocarpon (Gboma)	Y	N	Y	Y	N
African eggplant (Kade)	Y	Y	Y	Y	Y
Crown rot development at 7 days after stem inoculation					
Chilli pepper (Legon 18)	Y	Y	Y	Y	Y
Bell pepper (Yellow wonder)	Y	Y	Y	N	Y
Turkey berry (*S. torvum*)	Y	Y	Y	Y	Y
Tomato (cv. Pectomech)	Y	Y	Y	Y	Y
S. macrocarpon (Gboma)	Y	Y	Y	Y	Y
African eggplant (Kade)	Y	Y	Y	Y	Y

Note: Inoculum in the host range text was prepared using *F. elaeidis* isolate Oku015, *F. fredkrugeri* isolate Dzod03, *N. falciforme* isolate Adie04, *N. suttoniana* isolate Akun03 and *N. solani* isolate Abek02.
Abbreviations: N, absence of symptoms after inoculation; Y, plant developed symptoms after inoculation.

Accurate identification of *Fusarium* spp. requires a polyphasic approach that incorporates morphological observations and genetic/molecular characteristics (O'Donnell et al. 2022). This study used Btub2, Tef-1α and Rpb2 gene sequences to construct a multilocus phylogenetic tree to support the morphological identification. The multilocus phylogenetic effectively identified all fungal isolates up to the species level. Further, the analysis of individual genes using BLAST searches and phylogenetic approaches (data not shown) revealed that the *Tef-1α* and *Rpb2* loci outperformed *Btub2* in identifying the fungal species. Considering these findings and recommendations from comparable studies (O'Donnell et al. 2022; Sandoval-Denis and Crous 2018), it is crucial to recognise that *Btub2* sequencing alone may not be sufficient for the accurate identification of *Fusarium* and *Neocosmospora* species associated with a disease. The low discriminatory power of the *Btub2* gene is likely attributed to the detected genetic homogeneity among species and its rapid evolution rate (Stielow et al. 2015). *Tef-1α* and *Rpb2* genes in *Fusarium* taxa exhibit significant levels of sequence polymorphism among closely related species, enhancing their accuracy in inferring deep evolutionary relationships (Lombard et al. 2019; Sandoval-Denis and Crous 2018; Stielow et al. 2015). As a result, they have always been the first choice of many studies.

The pathogenicity tests conducted on the roots and stems of healthy AEPs showed that the five fungal species caused symptoms of crown rot and wilt, with varied levels of virulence depending on the infected host organ, fungal species and isolates. For example, *F. elaeidis* was the most virulent wilt-inducing agent upon root inoculation, whereas its effect on stems was minimal. *N. solani* and *N. suttoniana* were the most virulent when the stems were inoculated but not on the roots. These observations agree with previous studies documenting the influence of specific host organs on pathogen virulence (Gdanetz, Noel, and Trail 2021). The observed disparities in virulence may stem from factors, including the structural adaptation of pathogen to specific organs, genetic differences among fungal isolates (Lacaze and Joly 2020) and host-related factors such as variability in the expression of pathogenesis-related proteins, quantitative resistance and morphological adaptations (Akbar et al. 2018). These findings shed light on the dynamics of host–pathogen interactions during disease development and identify the plant organs most susceptible to infection, providing valuable insights for directing disease control efforts.

Moreover, because wilt and crown rot share similar aboveground symptoms and are generally difficult to distinguish under field conditions, it was challenging to identify the primary host organ infected in the wilting plants with crown rot symptoms. Present fungal isolations showed that *F. elaeidis* was exclusive to plants displaying wilt symptoms, while the other pathogenic species were commonly related to wilting plants with crown rot symptoms in the field. These results, together with the symptoms manifested by the distinct fungal species in our pathogenicity tests, strongly indicated that the wilt of AEP is caused by *F. elaeidis* infecting roots, while the three *Neocosmospora* species, along with *F. fredkrugeri* contributed to wilt by infecting plant stems (or primarily caused crown/stem rots). However, it was not possible to exclude *F. elaeidis* as a stem pathogen as well as exclude the three *Neocosmospora* species together with *F. fredkrugeri* as potential root pathogens of AEP because they may need a longer time and natural environmental conditions for the development of symptoms (Gaire et al. 2023). Further studies should be conducted in the natural environment to fully elucidate the relationships between fungal pathogens and symptom manifestation in AEP.

In this investigation, *F. elaeidis* and *N. falciforme* emerged as the predominant pathogens isolated from diseased AEPs. The dominance of *N. falciforme* in the Volta region, where *F. elaeidis* was notably absent and oil palm cultivation is infrequent, suggests the specificity of *F. elaeidis* to oil palm and highlights regional variations in pathogen prevalence. Also, the wide distribution of *F. elaeidis* across four of the five regions surveyed indicates that it is well established in Ghana, where rotations between oil palm and AEP are prevalent cropping practices (Nuertey, Ofori, and Asamoah 2001). These results underscore the significant role of agricultural practices in shaping pathogen distribution dynamics (Akbar et al. 2018). *F. elaeidis*, classified within the FOSC, is recognised as a global pathogen responsible for inducing wilt in oil palm (*Elaeis guineensis*) (Flood 2006), along with root and stem rot in *Alocasia longiloba* (Zhang et al. 2021) and sweet potato (De Mello et al. 2024).

Fusarium fredkrugeri, belonging to the *F. fujikuroi* species complex, has not been previously identified as a plant pathogen since its discovery in 2018 (Sandoval-Denis, Swart, and Crous 2018). During this study, one isolate of *F. fredkrugeri* was detected alongside *N. falciforme* in a field within the Volta region. The pathogenicity tests established *F. fredkrugeri* as exhibiting weak pathogenicity on the roots and moderate pathogenicity on the stems of AEPs, making the first documentation of its pathogenic behaviour on this host.

The host range assays demonstrated the susceptibility of chilli pepper, bell pepper, turkey berry, tomato and *S. macrocarpon* to selected isolates from the five fungal species. These results indicate that these hosts can become alternate or even the primary hosts for the tested isolates. Therefore, caution should be exercised when recommending these crops for rotation in AEP fields. Furthermore, while *F. elaeidis* and *F. fredkrugeri* have a restricted host range compared to the three *Neocosmospora* spp., which have been documented to infect a wide range of crops from various plant families (Sandoval-Denis and Crous 2018), the distribution of these pathogens, particularly *F. elaeidis*, in regions cultivating oil palm (Flood 2006) increases the likelihood of interactions with new plant species. Given that vegetables are commonly intercropped with oil palm during the juvenile stages (1–5 years) to provide supplementary income to farmers (Nuertey, Ofori, and Asamoah 2001), the present study underscores the importance of considering the potential expansion of *F. elaeidis* host range. Consequently, farmers may opt for resistant crops when selecting plants for oil palm cropping systems to mitigate the risk of fungal infection.

The previous identification of *Fusarium* species causing wilt disease of AEP in Ghana was only based on morphological characteristics, and the pathogenicity of these species could not be confirmed (Owusu et al. 2023). Therefore, by using molecular identification techniques, proving pathogenicity and sampling from more regions, the present study marks the first

comprehensive inquiry into the fungal agents causing the wilt of AEP in Ghana. This study is the first report of *F. elaeidis*, *F. fredkrugeri*, *N. falciforme*, *N. suttoniana* and *N. solani*, causing wilt and crown rot disease in Ghana.

In general, the prevalence of wilt in AEP fields may result from agricultural practices and farmer behaviour (Owusu et al. 2023; Akbar et al. 2018). AEP farmers in Ghana commonly exchange and reuse seeds from previous harvests to establish nurseries (Shafiwu, Donkoh, and Abdulai 2022). *Fusarium* spp. are soil-borne and seed-borne pathogens; therefore, seedlings raised from contaminated seeds are readily infected shortly after germination. Furthermore, the rising consumer demands in recent years have reduced crop rotations and increased continuous cropping of fields with a limited number of genetically diverse cultivars (Owusu et al. 2023). These agricultural practices are well known to promote the build-up and spread of inoculum, leading to the rapid development of wilt epidemics (Altınok and Can 2010). Thus, raising awareness among farmers about utilising certified seeds, introducing genetically diverse cultivars and implementing crop rotation programmes could help reduce the incidence of Fusarium wilt disease in AEP.

In summary, this study has characterised the fungal species associated with wilt and crown rot in AEP in Ghana and determined the potential host range of the identified pathogenic agents. The findings are valuable and considerably improve our understanding of the wilt disease aetiology and symptomatology in AEP. Moreover, they hold promise for informing the development of targeted disease control strategies, including crop rotations, and for facilitating the screening of eggplant genetic resources to identify suitable candidates for resistance breeding.

Acknowledgements

This research was funded by the Ministry of Foreign Affairs of Denmark through the project 'Building Vegetable Farmers Resilience to Climate Change', DFC project no: 19-04-AU. We thank George Nii Ankrah for his technical support in completing the screen house trials.

Conflicts of Interest

The authors declare no conflicts of interest.

Data Availability Statement

All the sequence data generated in this study are publicly available at GenBank (https://www.ncbi.nlm.nih.gov/genbank/). See Table S3 for accession numbers. Other data supporting the findings of this study are available from the corresponding author upon reasonable request.

References

Akbar, A., S. Hussain, K. Ullah, M. Fahim, and G. S. Ali. 2018. "Detection, Virulence and Genetic Diversity of *Fusarium* Species Infecting Tomato in Northern Pakistan." *PLoS One* 13: e0203613.

Altınok, H. H., and C. Can. 2010. "Characterization of *Fusarium oxysporum* f. sp. *melongenae* Isolates From Eggplant in Turkey by Pathogenicity, VCG and RAPD Analysis." *Phytoparasitica* 38: 149–157.

Boyaci, F., A. Unlu, and K. Abak. 2010. "Screening for Resistance to *Fusarium* Wilt of Some Cultivated Eggplants and Wild Solanum Accessions." In *XXVIII International Horticultural Congress on Science and Horticulture for People (IHC2010): International Symposium on New 935*, 23–27.

Cerkauskas, R. 2008. "Fusarium Stem Canker of Greenhouse Eggplant (*Solanum melongena* var. *esculentum*) in Ontario." *Canadian Journal of Plant Pathology* 30: 614–618.

Crous, P. W., L. Lombard, M. Sandoval-Denis, et al. 2021. "Fusarium: More Than a Node or a Foot-Shaped Basal Cell." *Studies in Mycology* 98: 100116.

Darriba, D., G. L. Taboada, R. Doallo, and D. Posada. 2012. "jModelTest 2: More Models, New Heuristics and Parallel Computing." *Nature Methods* 9: 772.

De Mello, J. F., A. C. da Silva Santos, A. C. de Queiroz Brito, et al. 2024. "Species Diversity of Fusarioid Genera Associated With Sweet Potato in Brazil, Including the Description of a New Species." *Plant Pathology* 73: 975–990.

Dereeper, A., V. Guignon, G. Blanc, et al. 2008. "Phylogeny. Fr: Robust Phylogenetic Analysis for the Non-Specialist." *Nucleic Acids Research* 36: W465–W469.

Drummond, A. J., M. A. Suchard, D. Xie, and A. Rambaut. 2012. "Bayesian Phylogenetics With BEAUti and the BEAST 1.7." *Molecular Biology and Evolution* 29: 1969–1973.

Flood, J. 2006. "A Review of Fusarium Wilt of Oil Palm Caused by *Fusarium oxysporum* f. sp. *elaeidis*." *Phytopathology* 96: 660–662.

Gaire, S. P., X. G. Zhou, Y. Zhou, J. Shi, and Y. K. Jo. 2023. "Identification and Distribution of Fungal Pathogens Associated With Seedling Blight of Rice in the Southern United States." *Plant Pathology* 72: 76–88.

Gdanetz, K., Z. Noel, and F. Trail. 2021. "Influence of Plant Host and Organ, Management Strategy, and Spore Traits on Microbiome Composition." *Phytobiomes Journal* 5: 202–219.

Glass, N. L., and G. C. Donaldson. 1995. "Development of Primer Sets Designed for Use With the PCR to Amplify Conserved Genes From Filamentous Ascomycetes." *Applied and Environmental Microbiology* 61: 1323–1330.

Hall, T. 1999. "BioEdit: A User-Friendly Biological Sequence Alignment Editor and Analysis Program for Windows 95/98/NT." *Nucleic Acids Symposium Series* 41: 95–98.

Han, M., K. N. Opoku, N. A. Bissah, and T. Su. 2021. "*Solanum aethiopicum*: The Nutrient-Rich Vegetable Crop With Great Economic, Genetic Biodiversity and Pharmaceutical Potential." *Horticulturae* 7: 126.

Hoang, D. T., O. Chernomor, A. Von Haeseler, B. Q. Minh, and L. S. Vinh. 2018. "UFBoot2: Improving the Ultrafast Bootstrap Approximation." *Molecular Biology and Evolution* 35: 518–522.

Horna, D., S. Timpo, and G. Gruère. 2007. "Marketing Underutilized Crops: The Case of the African Garden Egg (*Solanum ethiopicum*) in Ghana." 26.

Lacaze, A., and D. L. Joly. 2020. "Structural Specificity in Plant–Filamentous Pathogen Interactions." *Molecular Plant Pathology* 21: 1513–1525.

Leslie, B., and J. Summerell. 2006. *The Fusarium Laboratory Manual*. Ames, IA: Blackwell Publishing Professional.

Liu, Y. J., S. Whelen, and B. D. Hall. 1999. "Phylogenetic Relationships Among Ascomycetes: Evidence From an RNA Polymerse II Subunit." *Molecular Biology and Evolution* 16: 1799–1808.

Lombard, L., M. Sandoval-Denis, S. C. Lamprecht, and P. W. Crous. 2019. "Epitypification of *Fusarium oxysporum*–Clearing the Taxonomic Chaos." *Persoonia-Molecular Phylogeny and Evolution of Fungi* 43: 1–47.

Mui-Keng, T., and L. M. Niessen. 2003. "Analysis of rDNA ITS Sequences to Determine Genetic Relationships Among, and Provide a Basis for Simplified Diagnosis of, *Fusarium* Species Causing Crown rot and Head Blight of Cereals." *Mycological Research* 107: 811–821.

Nguyen, L.-T., H. A. Schmidt, A. Von Haeseler, and B. Q. Minh. 2015. "IQ-TREE: A Fast and Effective Stochastic Algorithm for Estimating Maximum-Likelihood Phylogenies." *Molecular Biology and Evolution* 32: 268–274.

Nuertey, B., K. Ofori, and T. Asamoah. 2001. "Performance of Food Crops Inter-Cropped With Oil Palm." *Journal of the Ghana Science Association* 3: 17–22.

O'Donnell, K., H. C. Kistler, E. Cigelnik, and R. C. Ploetz. 1998. "Multiple Evolutionary Origins of the Fungus Causing Panama Disease of Banana: Concordant Evidence From Nuclear and Mitochondrial Gene Genealogies." *Proceedings of the National Academy of Sciences of the United States of America* 95: 2044–2049.

O'Donnell, K., B. K. Whitaker, I. Laraba, et al. 2022. "DNA Sequence-Based Identification of *Fusarium*: A Work in Progress." *Plant Disease* 106: 1597–1609.

Owusu, E., C. Kwoseh, E. Osekre, and R. Akromah. 2023. "Incidence, Diversity and Distribution of *Fusarium* Wilt Pathogens of Eggplant in Some Major Growing Areas of Ashanti, Eastern and Volta Regions of Ghana." *Ghana Journal of Agricultural Science* 58: 118–127.

Reeb, V., F. Lutzoni, and C. Roux. 2004. "Contribution of RPB2 to Multilocus Phylogenetic Studies of the Euascomycetes (Pezizomycotina, Fungi) With Special Emphasis on the Lichen-Forming Acarosporaceae and Evolution of Polyspory." *Molecular Phylogenetics and Evolution* 32: 1036–1060.

Safikhani, N., B. Morid, and H. R. Zamanizadeh. 2013. "First Report of Fusarium Wilt of Eggplant Caused by *Fusarium oxysporum* f. sp. *melongenae* in Iran." *New Disease Reports* 28: 16.

Sandoval-Denis, M., and P. W. Crous. 2018. "Removing Chaos From Confusion: Assigning Names to Common Human and Animal Pathogens in *Neocosmospora*." *Persoonia-Molecular Phylogeny and Evolution of Fungi* 41: 109–129.

Sandoval-Denis, M., V. Guarnaccia, G. Polizzi, and P. W. Crous. 2018. "Symptomatic Citrus Trees Reveal a New Pathogenic Lineage in *Fusarium* and Two New *Neocosmospora* Species." *Persoonia-Molecular Phylogeny and Evolution of Fungi* 40: 1–25.

Sandoval-Denis, M., W. J. Swart, and P. W. Crous. 2018. "New *Fusarium* Species From the Kruger National Park, South Africa." *MycoKeys* 34: 63–92.

Schoch, C. L., K. A. Seifert, S. Huhndorf, et al. 2012. "Nuclear Ribosomal Internal Transcribed Spacer (ITS) Region as a Universal DNA Barcode Marker for Fungi." *Proceedings of the National Academy of Sciences of the United States of America* 109: 6241–6246.

Shafiwu, A. B., S. A. Donkoh, and A.-M. Abdulai. 2022. "The Welfare Impact of Improved Seed Variety Adoption in Ghana." *Journal of Agriculture and Food Research* 10: 100347.

Stielow, J. B., C. A. Levesque, K. A. Seifert, et al. 2015. "One Fungus, Which Genes? Development and Assessment of Universal Primers for Potential Secondary Fungal DNA Barcodes." *Persoonia-Molecular Phylogeny and Evolution of Fungi* 35: 242–263.

Tamura, K., and M. Nei. 1993. "Estimation of the Number of Nucleotide Substitutions in the Control Region of Mitochondrial DNA in Humans and Chimpanzees." *Molecular Biology and Evolution* 10: 512–526.

Tassone, M. R., P. Bagnaresi, F. Desiderio, et al. 2022. "A Genomic BSAseq Approach for the Characterization of QTLs Underlying Resistance to *Fusarium oxysporum* in Eggplant." *Cells* 11: 2548.

Thompson, J. D., D. G. Higgins, and T. J. Gibson. 1994. "CLUSTAL W: Improving the Sensitivity of Progressive Multiple Sequence Alignment Through Sequence Weighting, Position-Specific Gap Penalties and Weight Matrix Choice." *Nucleic Acids Research* 22: 4673–4680.

Toppino, L., G. Valè, and G. L. Rotino. 2008. "Inheritance of Fusarium Wilt Resistance Introgressed From *Solanum aethiopicum* Gilo and Aculeatum Groups Into Cultivated Eggplant (*S. melongena*) and Development of Associated PCR-Based Markers." *Molecular Breeding* 22: 237–250.

Villesen, P. 2007. "FaBox: An Online Toolbox for Fasta Sequences." *Molecular Ecology Notes* 7: 965–968.

Xu, X., R. Minja, E. B. Kizito, et al. 2024. "Amplicon Sequencing Identified a Putative Pathogen, *Macrophomina phaseolina*, Causing Wilt in African Eggplant (*Solanum aethiopicum*) Grown in Tanzania and Uganda." *Frontiers in Agronomy* 5: 1300324.

Zhang, Y., C. Chen, J. Zhao, et al. 2021. "*Fusarium elaeidis* Causes Stem and Root Rot on *Alocasia longiloba* in South China." *Pathogens* 10: 1395.

Supporting Information

Additional supporting information can be found online in the Supporting Information section.